Surface Science

Micro/Nanostructure

Growth kinetics in ultrathin organic films
Fink, R., Th. Schmidt, U. Groh, E. Umbach

Observation of microphase segregation in binary polymer brushes
Usov, D., C. Froeck, A. Scholl, S. Minko, M. Stamm

Photoemission electron microscopy and x-ray magnetic circular dichroism of $Fe_xNi_{(1-x)}$ thin films on Cu(111)
Sato, Y., T.F. Johnson, S. Chiang, X.D. Zhu, D.P. Land, J.A. Giacomo, F. Nolting, A. Scholl

Resonant x-ray fluorescence holography: Three-dimensional atomic imaging in true color
Omori, S., L. Zhao, S. Marchesini, M. A. Van Hove, C. S. Fadley

Spin-resolved electronic structure studies of ultrathin films of Fe on singular and vicinal GaAs
Spangenberg, M., E.A. Seddon, E.M.M. McCash, T. Shen, S.A. Morton, D. Waddill, J. Tobin

Growth kinetics in ultrathin organic films

R. Fink, Th. Schmidt, U. Groh, E. Umbach
Experimentelle Physik II, Universität Würzburg, Am Hubland, D-97074 Würzburg, Germany

INTRODUCTION

Thin films of large organic molecules are interesting model systems with respect ot their technological importance. Nowadays, more and more applications of such materials are reported, e.g. in microelectronics, light-emitting devices, or photosensors. However, for many applications, the conventional films prepared by sublimation in high vacuum without control of the structural properties, are polycrystalline with lots of structural defects, which drastically influence the electronic and optical properties of such devices. Structural order becomes even more important in devices, where the formation of well-defined heterointerfaces of organic substances is preferred, e.g., when combining p- and n- conducting organic materials.

Previous experiments have demonstrated the influence of the metal-organic interface on the formation of different superstructures which extend into the third dimension and may lead to ideal epitaxial film growth. However, although polymorphic phases are known for many organic materials, it is difficult to optimize the growth conditions with respect to long-range ordered homogeneous films.

EXPERIMENT AND RESULTS

We have used XPEEM to investigate the film morphologies of ultrathin NTCDA films on Ag(111) for different growth conditions. NTCDA has been chosen since the molecular orientation in thin films can easily be manipulated by variation of the substrate temperature between 200 K and room temperature [1]. The experiments were performed at PEEM2 (BL 7.3.1.1). The Ag substrate was prepared by repeated sputter-annealing cycles. The NTCDA films were grown by vacuum sublimation in a separate preparation chamber. We recorded images for various photon energies to extract local NEXAFS/XANES spectra.

Fig. 1 shows XPEEM images two differently prepared films. The nominal film thickness varies by about 50 per cent for the two samples; the evaporation rate was estimated to about 1 monolayer per minute. Two different growth modes were detected: at elevated temperatures of 320 K the prominent structures are rectangularly shaped dark areas on a bright background. The high emission intensity is due to emission from the Ag substrate which is favored under these conditions for all photon energies, since the secondary electron yield (image formation in XPEEM without energy filter is primarily due to secondaries with low kinetic energy !) for Ag is much larger than for the organic compound. The dark areas are identified as NTCDA microcrystals. A closer inspection of their relative orientation yield angles of 60 and 120 degrees for their long axis. Thus, we may directly conclude that the underlying Ag(111) substrate, which has a 6-fold symmetry (with respect to its top layer) influences the growth direction.

Local NEXAFS spectroscopy clearly yields π^*-resonances characteristic for NTCDA monolayers in a chemisorbed surrounding [2] for areas in between the microcrystals. This indicates a Stranski-Krastanov growth mode, which is consistent with the relatively strong interaction between NTCDA and the metal substrate. LEED investigations reflect the diffraction

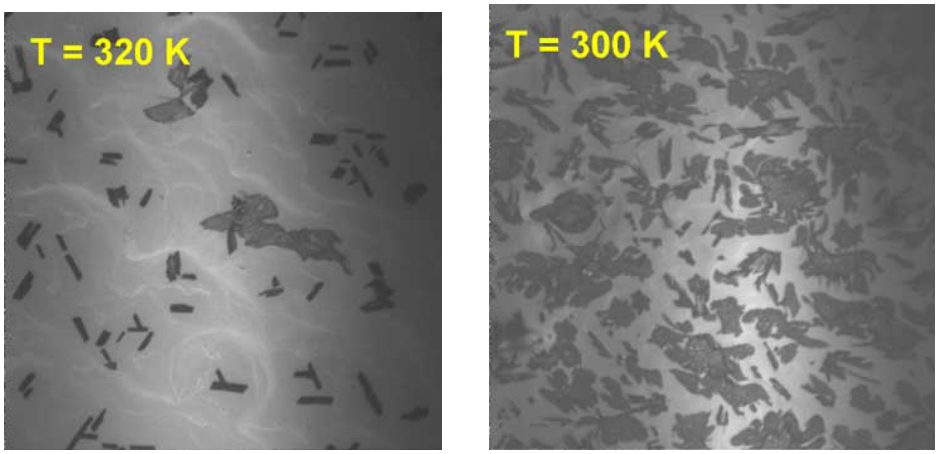

Fig. 1: NTCDA films (nominal thickness around 5 monolayers) adsorbed on Ag(111) at 320 K (left) and 300 K (right). Bright stripes correspond to bunched steps. Image size: 60 x 60 μm², hν = 540 eV.

pattern of the monolayer species (for saturation coverage [3]) and support the finding from the NEXAFSspectra obtained from the bright areas.

For lower temperatures (300 K), the image looks very different. Instead of regularly shaped domains we find fractal growth of organic islands (Fig. 2, right). Compared to the film growth at elevated temperatures there is a much higher density of islands which is due to the smaller diffusion length. In addition, the individual islands are not homogenous. We attribute this finding to the mismatch of the structural parameters. So far, no experimental evidence is found for epitaxial growth of NTCDA/Ag(111). The LEED pattern in this case is diffuse and shows only broad diffraction spots consistent with the small domains. From other experiments (HREELS) there are indications that this film has a different molecular orientation compared to the high- and low-temperature phases, respectively [1].

From the present geometric setup at PEEM2 it is unfortuntely not possible to derive the local molecular orientation from NEXAFS dichroism. Future experiments will focus on in-situ prepared films to investigate the growth kinetics during adsorption and thus allow the investigation of adsorption processes on a real-time scale. Proper image analysis may give direct access to diffusion parameters (diffusion length, activation energies). In this respect, XPEEM will offer new opportunities and thus overcome present limitation by scanning probe or laterally averaging spectroscopic techniques.

REFERENCES

[1] D. Gador, C. Buchberger, R. Fink, and E. Umbach, Europhys. Lett. **41**(2), 213 (1998).

[2] D. Gador, Y. Zou, C. Buchberger, M. Bertram, R. Fink, and E. Umbach, J. Electr. Spectr. Rel. Phenom. **101-103**, 529 (1999).

[3] R. Fink, D. Gador, Y. Zou, E. Umbach, Phys. Rev. B **60,** 2818 (1999).

This work was supported by the Bundesminister für Bildung und Forschung, contracts 05SL8WW18. We gratefully acknowledge experimental support by A. Scholl and A. Doran during the experiments at PEEM2.

Principal investigator: Rainer Fink. Experimentelle Physik II, Universität Würzburg.
Email: raifi@physik.uni-wuerzburg.de Telephone: +49-931-888-5163.

Observation of microphase segregation in binary polymer brushes

D. Usov[1], C. Froeck[1], A. Scholl[2], S. Minko[1], M. Stamm[1]
[1]Institut for Polymer Research Dresden, Hohe St. 6, 01069 Dresden, Germany
[2]Advanced Light Source, Ernest Orlando Lawrence Berkeley National Laboratory,
University of California, Berkeley, California 94720, USA

INTRODUCTION

The basic idea is creation of smart polymer layers with switching properties such as wetting behavior, adhesion, interaction with biological objects, and permeability of membranes. Such polymer layers can find their application in many areas such as information recording, sensors, self-cleaning clothes covering, nanodevices, in medicine and biological science for mimicking living cell membranes, for selective adsorption and recognition of proteins and living cells. The route, how to make this dream true, comprises binding to solid substrate different polymers[1] or block-copolymers and switch the film structure in such a way, that this film responding to various external stimuli can adopt particular desired properties: hydrophylic/hydrophobic balance, selective adsorption of particular molecules, etc.

We are currently studying model layers composed of two different (hydrophilic and hydrophobic) linear polymers covalently grafted to silicon substrates which can be switched upon exposure to solvents of different thermodynamical quality[1]. The grafting density is so high that the distance between grafting points of neighbor polymer molecules is much (about 10 times) shorter than the size of the polymer coils (mean distance between chain ends in theta-conditions). Therefore the polymer coils interact with their neighbors and are elongated in the direction perpendicular to the substrate. All the conformational changes are cooperative. Such regime is known as the brush regime. If such a binary polymer brush is exposed to a selective solvent which good for the first brush polymer and poor for the second one the first polymer swells and occupies the top layer while the second polymer collapses and occupies the bottom layer near the substrate. If the solvent is replaced by another one with opposite selectivity the brush passes to a state inverse with respect to the previous one. In a solvent good for both polymers they both are present on the top of the layer. The time of solvent evaporation upon drying by nitrogen flow is much smaller than the time for morphology transformation. The morphologies after treatment in a particular solvent are reproducible and reversibly switch upon changing the solvent. We made the assumption that the spacial distribution of the polymers in the dry state after exposition to a solvent is a fingerprint of their distribution under the solvent[2].

The polymers are usually incompatible but only microphase segregation takes place because each polymer chain is chemically bound to a substrate with one end. The size of the aggregates is limited by the chains` length. Two limiting types of morphologies can be distinguished: the layered phase with only perpendicular phase segregation and the “ripple” phase with lateral segregation. Analytical studies of the microphase segregation in binary brushes under melt conditions and in various solvent conditions were done. Self consistent field calculations made by Marcus Müller[2] predict for binary polymer brushes in a solvent good for both components existence of the “ripple” phase consisting of parallel lying cylinders with alternating enrichment by each brush component. For the case of a selective solvent an existence of the “dimple” phase is predicted where the worse soluble polymer forms round clusters and the other polymer occupies the area around them. Experimental observation of microphase segregation in binary

polymer brushes was performed using facilities of the Ernest Orlando Lawrence Berkeley National Laboratory and was briefly reported elsewhere[2].

RESULTS

We synthesized binary polymer brushes by radical polymerization on a Si surface using for the grafting of the second polymer the residual azo-initiator on the surface[1]. The brush components were polystyrene with 25% of fully fluorinated aromatic rings (P(S-co-FS)) and polymethylmethacrylate (PMMA).

We observed the reversible morphology switching from elongated species after treatment in toluene to round clusters after exposition to acetone with Atomic Force Microscopy (AFM) (see Fig.1).

We investigated the chemical composition of the brushes` top layers (≤5 nm) after exposition to toluene and acetone applying X-Ray Photoelectron Emission Microscopy (XPEEM). The difference between the carbon peaks in Near Edge X-Ray Absorption Fine Structure spectra (NEXAFS) for polystyrene (286.1 eV) and PMMA (289.3 eV)[3] was used to distinguish between the polymers. We observed the inverse contrast of elongated species at the XPEEM images recorded at 286.1 eV and 289.3 eV for the brush exposed to toluene (see Fig.2). We were unable to find any chemical contrast at the XPEEM images for the brush exposed to acetone due to a strong signal distortion caused by highly rough brush surface.

The integral NEXAFS spectra were recorded from the surfaces of the brushes after exposure to toluene, acetone, and after annealing at 150ºC for 24 hours in vacuum. The water contact angle on the same surfaces was measured. The chemical composition of the top layers of the brushes was calculated and similar results were obtained from these two methods. The top layer of the brushes was enriched with P(S-co-FS) after exposition to toluene and after annealing and with PMMA after exposition to acetone (see Table 1).

We conclude qualitative agreement of the experimentally observed morphologies with the self consistent field calculations.

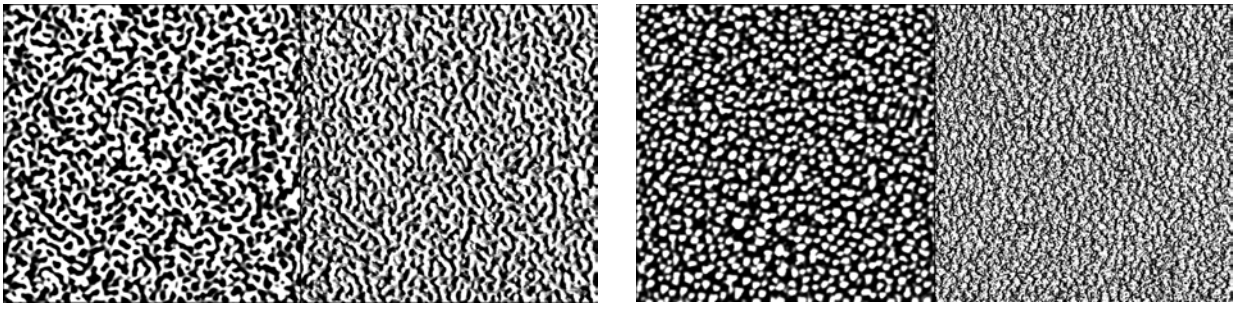

Figure 1. AFM tapping mode images 5x5 μm of the P(S-co-FS)/PMMA brush after exposure to toluene (A,B) and acetone (C,D): topography (A,C), phase (B,D) at 50% set-point ratio.

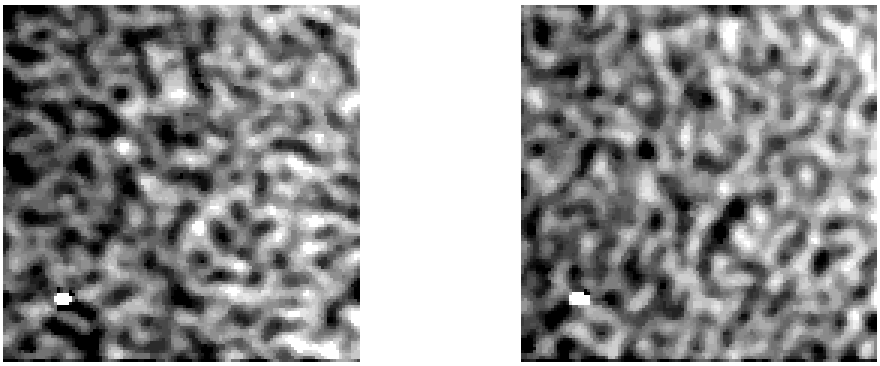

A B

Figure 2. XPEEM images 3x3 μm of the PSF-PMMA1 brush after exposure to toluene showing contrast between C edges of both polymers at 286,1 eV (A) and 289,2 eV (B) for PS and PMMA, respectively.

Table 1. Fraction of PMMA in the top layer of the brushes after exposure to solvents and annealing.

Sample	Contact angle, deg	PMMA fraction in the top layer, % calculated from the contact angle	PMMA fraction in the top layer, % calculated from the XPEEM data
P(S-co-FS)	96.6	0	0
PMMA	76.1	100	100
P(S-co-FS)/PMMA brushes after:			
exposure to toluene	90	32	29
exposure to acetone	81	76	78
in vacuum, at 150°C for 10h	91.5	25	20

REFERENCES

1. Alexander Sidorenko, Sergiy Minko, Karin Schenk-Meuser, Heinz Duschner, and Manfred Stamm, *Langmuir*, Vol. 15, N 24, **1999**, p. 8349.
2. S. Minko, M. Müller, D. Usov, A. Scholl, C. Froeck, and M. Stamm, *Physical Review Letters*, Vol. 88, N 3, **2002**, 035502.
3. Adam Hitchcock, McMaster University, 1280 Main Street West, Hamilton, Ontario, L8S 4L8, Canada, E-mail: aph@mcmaster.ca, private communication.

This work was supported by the Institute for Polymer Research Dresden, Hohe St. 6, 01069 Dresden, Germany and the European Graduate College "Advanced Polymeric Materials", Technical University Dresden, 01062 Dresden, Germany.

Principal investigator: Manfred Stamm, Institute for Polymer Research Dresden, Hohe St. 6, 01069 Dresden, Germany, E-mail: stamm@ipfdd.de, tel. +49 (351) 4658 224, web site: www.ipfdd.de.

Photoemission Electron Microscopy and X-Ray Magnetic Circular Dichroism of $Fe_xNi_{(1-x)}$ Thin Films on Cu(111)

Y.Sato[1], T.F.Johnson[1], S.Chiang[1], X.D.Zhu[1], D.P.Land[2], J.A.Giacomo[1]
F.Nolting[3], and A.Scholl[3]

[1]Dept. of Physics, University of California, Davis, CA 95616
[2]Dept. of Chemistry, University of California, Davis, CA 95616
[3]Advanced Light Source, Lawrence Berkeley National Laboratory,Berkeley, CA 94720

INTRODUCTION

Our research focuses on controlling the structure, composition and the resultant magnetic properties of metal alloy thin film growth at the atomic level. Better understanding and control of surface/interface magnetism is relevant to the application of the giant magneto-resistive effect to read heads for magnetic recording. We have studied $Fe_xNi_{(1-x)}$ alloy thin films for their technological relevance to the above mentioned technology. The dependence of the magnetism on the stoichiometry x is one of the questions of interest. In addressing this problem, the structure of the thin film must be also considered. In terms of crystal structure, a well known "Invar effect" exists in bulk FeNi alloy because of structural incompatibilities of the two elements. Pure Fe is stable in bcc phase whereas pure Ni has fcc structure. A bulk alloy containing more than 65% Fe transforms to bcc by a Martensitic transformation, and the magnetization falls to zero. In thin film alloys, the problem may become more complex because of the effect of substrate structure and interface properties. On the other hand, how this structural change affects the magnetic order in the film is not well known. A simultaneous study of film structure, magnetic structure and magnetism is needed to better understand the system.

Several studies on $Fe_xNi_{(1-x)}$ alloy thin films have been reported[1,2,3,4]. Information on the growth, structure, and magnetic moments as a function of thickness and concentration has been obtained using various techniques such as low energy electron diffraction (LEED), reflection high energy electron diffraction (RHEED), photoelectron diffraction, surface magneto optical Kerr effect (SMOKE), X-ray magnetic linear dichroism (XMLD), Mossbauer spectroscopy, and superconducting quantum interference device (SQUID) magnetometry. We have used the photoemission electron microscope (PEEM2) at the Advanced Light Source (beamline 7.3.1.1) to study this film system. PEEM has the unique capability of imaging the film's magnetic structure with high spatial resolution and elemental specificity. Simultaneously, quantitative magnetic information can be obtained using magnetic circular dichroism in X-ray absorption spectroscopy. At two different thicknesses, we have made sixteen samples and studied the dependence of magnetic structure on varying Fe concentration and substrate quality (x = 0, 0.28, 0.55,0.6, 0.66, 0.74, 1.0 at 10Å≅5ML, x = 0.9, 0.25, 0.33, 0.42, 0.5, 0.55, 1.0 at 20Å ≅10ML). We have observed clear ferromagnetic domain structures of the film on a Cu(111) surface for $x \leq 0.60$ at room temperature.

RESULTS

Samples with high Fe content (x=0.66, 0.74 at 5ML) have been observed to be non-magnetic at room temperature. All other alloy samples ($x \leq 0.6$, 5ML and 10ML) showed clear ferromagnetic contrast. This trend of reduction in Curie temperature at higher Fe concentration is also observed by spin resolved photoemission spectroscopy measurements carried out at the Advanced Light Source (beamline 7.0.1.2). A pure Ni film at 5ML thickness was non-magnetic at room temperature. According to a SMOKE measurement, 5ML is approximately the thickness where the Curie temperature becomes less than room temperature for Ni/Cu(111)[5].

Fig. 1 shows typical ferromagnetic images with a 12μ m field of view for a 5ML thick $Fe_{0.6}Ni_{0.4}$ film on Cu(111). Each image is obtained by dividing an image acquired at the L3 Fe (or Ni) edge by one acquired at the L2 Fe (or Ni) edge. The images show alignment of the magnetic domains for

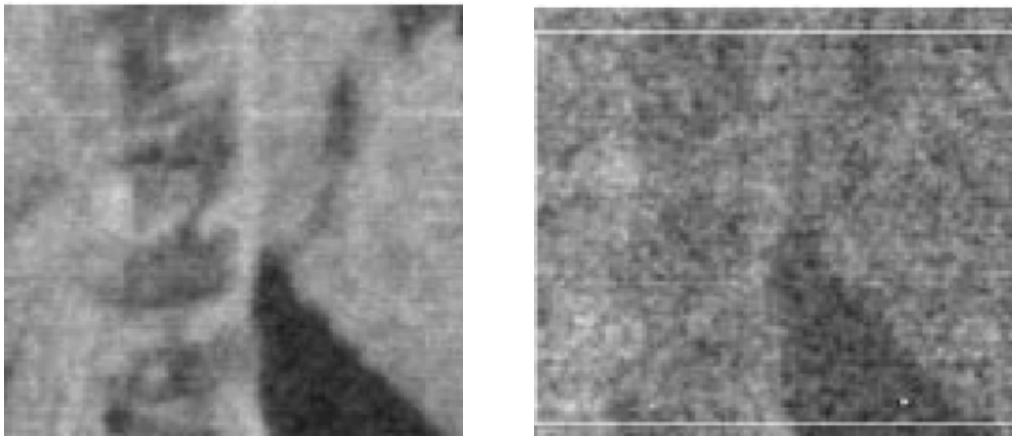

Fig. 1. XMCD ferromagnetic images with a 12μ m field of view for a 5ML thick $Fe_{0.6}Ni_{0.4}$/Cu(111). Left: Fe XMCD contrast, Right: Ni XMCD contrast.

Fe and Ni, suggesting that Fe and Ni form a good alloy on this surface. By comparing the images shown in Fig. 2 and Fig. 3, we find a clear dependence of the domain structures on film thickness and substrate quality. Fig. 2 shows magnetic contrast images of 5ML alloy films on a mechanically polished substrate. On these samples, observed magnetic structures appear to correlate to surface topographic features. No regular apperance of domain structure was seen. Comparison of the image at the pre-absorption edge, which shows only topographic contrast, with the magnetic contrast image clearly shows the correlation between surface structural features and the formation of magnetic domains. An experiment showed that magnetic contrast observed at room temperature disappears gradually upon heating. Contrast is recovered again as the sample temperature is lowered below the Curie temperature. This also confirms the relation between domain structure and surface geometric structures. These observations are consistent for each 5ML sample analyzed. In contrast, for 10ML films on an electropolished substrate as shown in Fig. 3, pinning due to surface defects is observed less frequently. Magnetic structures and textures appear to be more uniform and the sizes of the structures were smaller and on the order of 1-3μ m. At the alloy composition of x=0.44, regular, periodic appearance of larger domain structures (5-10μ m width and 70μ m length), defined by 180º domain walls, are observed, as shown in Fig. 4. By observing the two images shown in Fig. 4, we conclude that alloy film at this composition and thickness show in-plane magnetization.

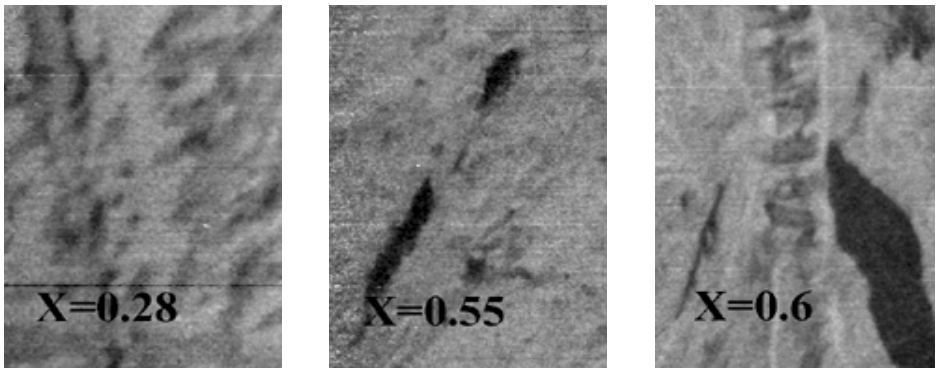

Fig. 2. XMCD ferromagnetic images with H22μ m×V30μ m field of view for 5ML films with varying Fe composition x.

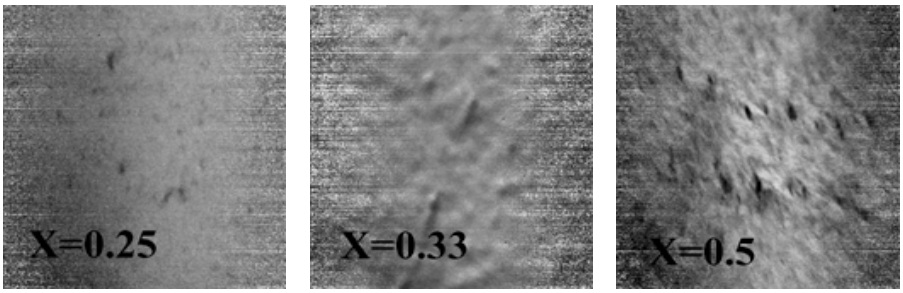

Fig. 3. XMCD ferromagnetic images with H65μ m×V65μ m field of view for 10ML films with varying Fe composition x.

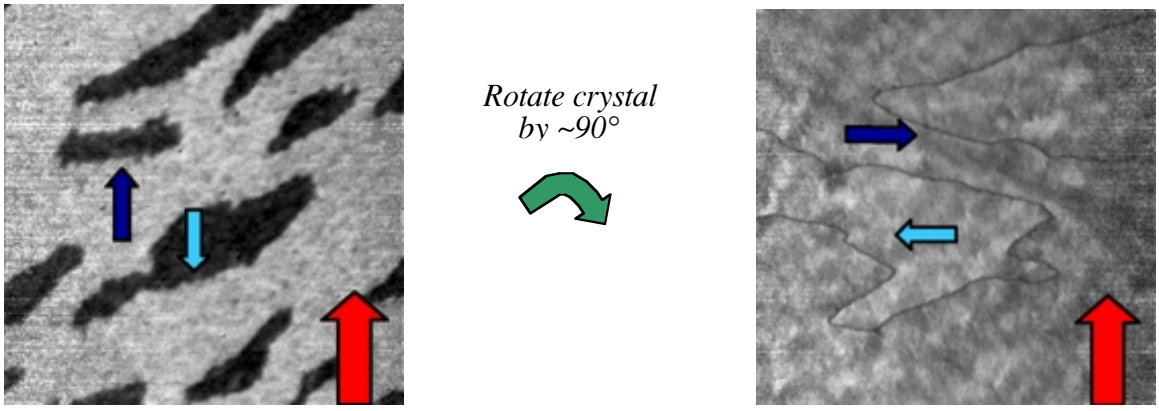

Fig. 4. XMCD ferromagnetic images with Right: H45μ m×V45μ m and Left: H45μ m×V45μ m field of view for 10ML thick $Fe_{0.56}Ni_{0.44}$/Cu(111). Smaller arrows indicate the magnetization direction and larger arrows show the direction of the incident photon momentum.

REFERENCES

1. F.O.Schumann, S.Z.Wu, G.J.Mankey, and R.F.Willis *Phys. Rev. B* **56** 2668 (1997)
2. F.O.Schumann, R.F.Willis, K.G.Goodman, and J.G.Tobin *Phys. Rev. Lett.* **79** 5166 (1997)
3. J.W.Freeland, I.L.Grigorov, and J.C.Walker *Phys. Rev. B.* **57** 80 (1998)
4. R.Schellenberg, H.Meinert, N.Takahashi, F.U.Hillebrecht, and E.Kisker *J. App. Phys.* **85** 6214 (1999)
5. R.Zhang, and R.F.Willis *Phys. Rev. Lett.* **86** 2665 (2001)

This work was supported by the Campus Laboratory Collaboration Program of the University of California Office of the President and by the Director, Office of Energy Research, Office of Basic Energy Sciences, of the U.S. Department of Energy under Contract No. DE-AC03-76SF00098.

Principal investigator: Shirley Chiang, Department of Physics, University of California, Davis, CA 95616-8677. Email: chiang@physics.ucdavis.edu. Telephone: 530-752-8538.

Resonant X-ray Fluorescence Holography: Three-Dimensional Atomic Imaging in True Color

S. Omori[1,2,#], L. Zhao[1,3], S. Marchesini[1], M. A. Van Hove[1,3,4], and C. S. Fadley[1,3]

[1] Materials Sciences Division, Lawrence Berkeley National Laboratory, Berkeley, California 94720
[2] Institute of Industrial Science, University of Tokyo, Tokyo 153-8505, Japan
[3] Department of Physics, University of California, Davis, California 95616
[4] Advanced Light Source, Lawrence Berkeley National Laboratory, Berkeley, California 94720
[#]Present address: Sony Research, Kawasaki, Japan

X-ray fluorescence holography (XFH) is a relatively new experimental tool for directly determining the local three-dimensional atomic structure around a given type of atom [1-4]. This element-specific method is based on the same concept as photoelectron holography [5], but detects instead fluorescent x-ray photons.

In the first type of XFH to be demonstrated experimentally [1a], one measures the interference between the fluorescent radiation directly emitted by the excited atoms and additional wave components of the same radiation scattered by various near-neighbor atoms. It is thus necessary to measure a given fluorescent intensity as a function of the direction of emission over as large a solid angle as possible. This method, for which the fluorescent atoms inside the sample act as sources and the intensity is measured in the far field, has been termed normal x-ray fluorescence holography (XFH) [2] or more specifically "direct XFH". In parallel with the first direct XFH experiment, Gog et al. [2a] proposed and demonstrated a different approach (termed multiple energy x-ray holography (MEXH) or "inverse XFH") by applying the optical reciprocity principle and exchanging the roles of source and detector. In this case, the fluorescent atoms inside the sample become the detectors for the net field produced by the interference of the incident x-ray beam and the components of this beam that are scattered by near-neighbor atoms. With present detection systems, MEXH is faster, as the incident beam can be very intense (e.g. emitted directly from a beamline monochromator or an undulator harmonic), and one can furthermore in principle detect all of the fluorescence emitted above the sample surface. Here, one is thus measuring the total fluorescence yield of a given atomic transition as a function of the direction of the incident x-ray beam. Being able to measure at multiple energies also results in images with less aberration due to twin-image effects and other non-idealities [2,5,6]. Recent XFH/MEXH studies have demonstrated the ability to image a first-row element in the presence of a transition metal [3], and to study the local atomic environment in a quasicrystal, even though translational periodicity is lacking for such a system [4]. Current experiments are by and large detector-limited as to the speed of data acquisition. In the ALS Compendium of 2000, we have discussed a project that has successfully measured the first MEXH holograms and holographic atomic images at the ALS [7].

Even though XFH and MEXH in their current formulations offer powerful methods to probe the local atomic structure around a given atom, there still remains one deficiency: the techniques may be element-specific for the central fluorescing atom in the structure (a quality they share with extended x-ray absorption fine structure (EXAFS)), but there is no simple way to determine the

near-neighbor atomic identities. Use can be made of the differences in non-resonant x-ray scattering strengths between different atoms (as is done with differences in electron scattering strength in EXAFS), but this is only unambiguous when atomic numbers are relatively far apart, as recently illustrated for the case of O and Ni in NiO [3]. In the present work, we propose a significant improvement to MEXH, resonant x-ray fluorescence holography (RXFH), that should enable the direct discrimination of different atoms in reconstructed images, even for the most difficult cases where atomic numbers of elements involved are very close together. It is in this sense that we can finally speak of atomic images "in true color" [8].

The principle of RXFH is discussed here for the example of a binary compound of AB_3 type with close atomic numbers, specifically $FeNi_3$, for which $Z_{Ni} - Z_{Fe} = 2$ and the fractional change in atomic number is only ~0.08 [8]. The central fluorescing atom of the reconstructed images is always chosen to be atom *A* (Fe in this case), and the anomalous dispersion associated with an absorption edge for element *B* (Ni in this case) is used to selectively image atoms *B* surrounding the central atom. In the usual implementations of MEXH in which both atoms *A* and *B* are to be equally imaged, the incident x-ray energies *E* are usually chosen in such a way that they are close enough to E_{abs}^{A}, the absorption edge of element *A*, for the efficient excitation of fluorescent x-rays from *A*, but also far enough from both E_{abs}^{A} and any edges E_{abs}^{B} of atom B that the anomalous dispersion terms in the x-ray scattering factors for *A* and *B* are not significant. In RXFH, by contrast, we will choose several *E*'s in the vicinity of an absorption edge E_{abs}^{B} of element *B*. The basic idea here is thus similar to that of multiple-wavelength anomalous diffraction (MAD) for phase determinations in conventional x-ray diffraction studies, but with the significant difference that there is from the outset no phase uncertainty in MEXH.

Making use of experimentally determined x-ray scattering factors for Fe (non-resonant) and Ni (resonant), as shown in Fig. 1, we have thus theoretically simulated holograms [6b] for a large cluster of atoms representing the $FeNi_3$ lattice as the Fe Kα fluorescence at 6.4 keV is monitored while scanning through the Ni K edge at about 8.3 keV [8]. As a first trial set of data, we have finally obtained MEXH and RXFH images based on the three energies shown in Fig. 2: below, on, and above the Ni K edge. One promising procedure for imaging in RXFH is shown elsewhere [8] to be using two difference holograms for E_1-E_2 and (with reversed sign) E_3-E_2. Fig. 2 shows the $FeNi_3$ crystal structure, together with normal MEXH images and RXFH images from these difference holograms. Fig. 2 makes it clear that the Ni-atom images are strongly suppressed in the RXFH images, thus suggesting this as a new approach in x-ray fluorescence holography for identifying near-neighbor atoms to a given type of fluorescent emitter.

In conclusion, resonant x-ray fluorescence holography should make it possible to obtain additional information on near-neighbor chemical identities that would lead to a much more complete structural characterization of any system, particularly one in which possible compositional disorder on the nm scale is present, and thus to a much broader applicability for nanoscale materials characterization. Future experiments at the ALS will explore this approach experimentally.

REFERENCES

[1] (a) M. Tegze, G. Faigel, Nature 380 (1996) 49; (b) (b) G. Faigel and M. Tegze, *Rep. Prog. Phys.* **62** (1999) 355.

[2] (a) T. Gog, P.M. Len, G. Materlik, D. Bahr, C.S. Fadley, C. Sanchez-Hanke, Phys. Rev. Lett. **76** (1996) 3132; (b) P.M. Len, C.S. Fadley, and G. Materlik, in X-ray and Inner-Shell Processes: 17th International Conference, R.L. Johnson, H. Schmidt-Böcking, and B.F. Sonntag, Eds., AIP Conference Proceedings, No. 389 (AIP, New York, 1997) p. 295.
[3] M. Tegze, G. Faigel, S. Marchesini, M. Belakhovsky, O. Ulrich, Nature 407, (2000) 38.
[4] S. Marchesini, et al., Phys. Rev. Lett. 85, (2000), 4723-6
[5] G.R. Harp, D.K. Saldin, B.P. Tonner, Phys. Rev. Lett. 65 (1990) 1012; plus more recent work at the ALS by P.M. Len et al. Phys. Rev. B **59** (1999) 5857
[6] (a) P.M Len, Ph.D. thesis, University of California at Davis (1997) and (b) simulation and imaging software described at http://electron.lbl.gov/holopack/holopack.html.
[7] S. Marchesini, L.Zhao, L. Fabris, M. W. West, J. Bucher, D. K. Shuh, W. C. Stolte, M. J. Press , A.S. Schlachter, Z. Hussain, and C. S. Fadley, ALS Compendium of Abstracts 2000: http://alspubs.lbl.gov/AbstractManager/uploads/00135.pdf.
[8] S. Omori, L. Zhao, S. Marchesini, M.A. Van Hove, and C.S. Fadley, Phys. Rev. B **65** (2002) 014106.

This work was supported by the U.S. Department of Energy, Office of Science, Office of Basic Energy Sciences, Materials Sciences Division, under Contract No. DE-AC03-76SF00098..

Principal investigator: Stefano Marchesini, Materials Sciences Division, Lawrence Berkeley National Laboratory. Email: marchesini@lbl.gov. Telephone: 510-486-4581.

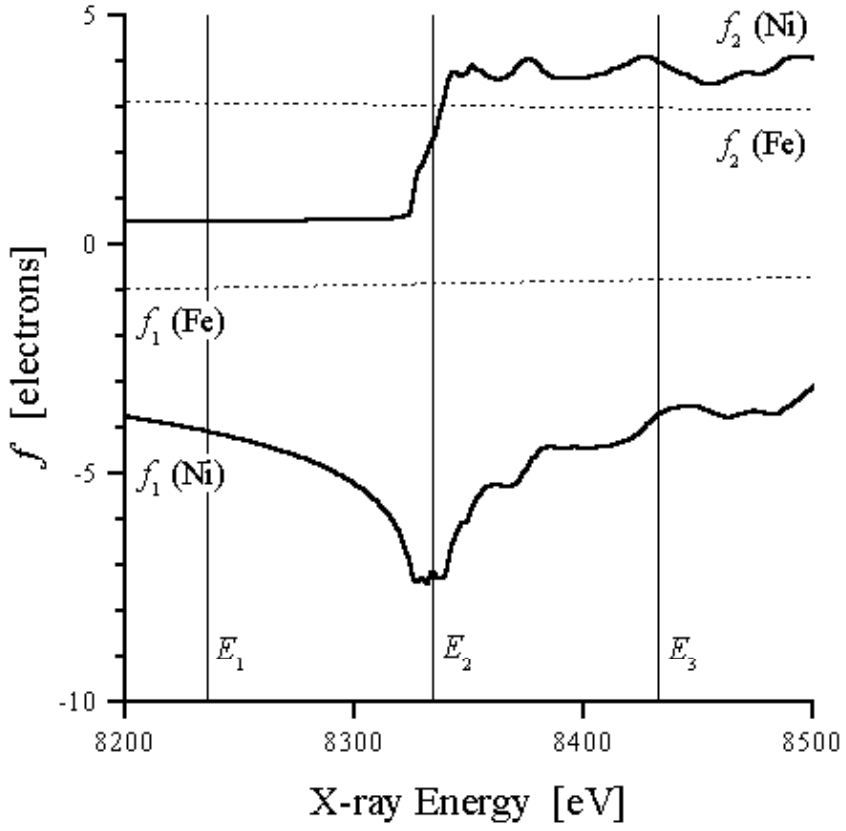

Fig. 1-- The atomic x-ray scattering factors f_1 and f_2 for Fe (dotted lines) and Ni (solid lines) as a function of x-ray energy around the *K* edge of Ni. The overall scattering factor is given by $f_{Atom} = f_0(\theta) + f_1 - if_2$, with $f_0(\theta)$ the form factor. The three energies used for the simulations of E_1, E_2 and E_3 are indicated by vertical solid lines and correspond to 8235 eV, 8334 eV, and 8433 eV, respectively.

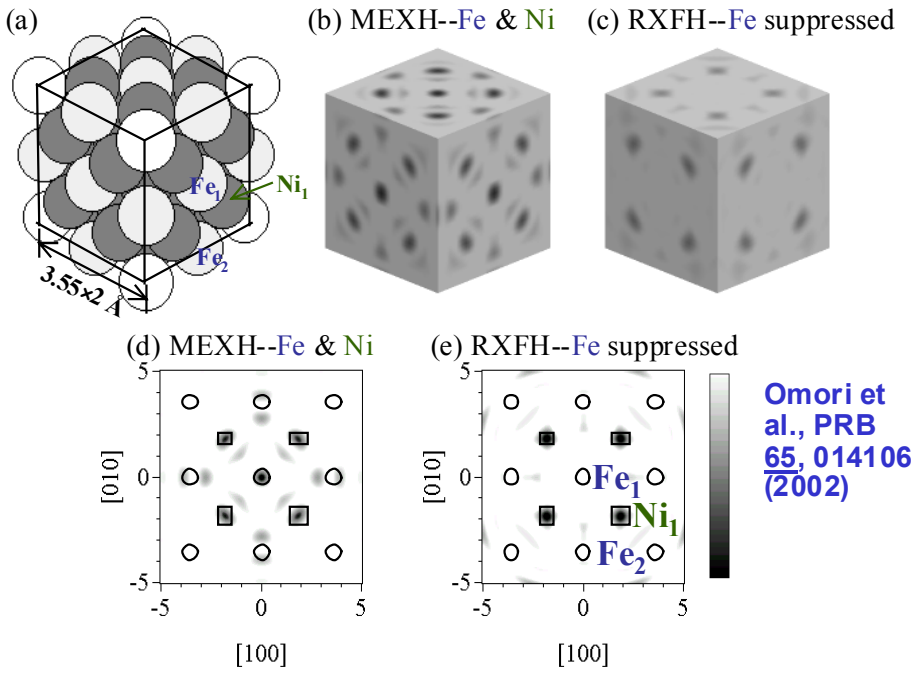

Fig. 2-- Comparison of multi-energy inverse x-ray fluorescence holographic images based on the negative of the real part of images generated using both the standard inversion algorithm (MEXH) and resonant holography (RXFH) based on two difference images (E_1-E_2 and E_3-E_2). These images are based on single-scattering cluster simulations of holograms [6b] at the three energies E_1, E_2 and E_3 for an $FeNi_3$ crystal containing about 10,000 atoms. (a) Near-neighbor atomic model of $FeNi_3$ for comparison to the reconstructed images in (b) and (c) and including 8 unit cells with the lattice constant of 3.55 Å. Fe atoms are lighter gray, and Ni atoms darker gray. The unique types of Fe and Ni atoms observed in (b) are labelled as Fe_1, Fe_2 and Ni_1. (b) Three dimensional reconstructed image from MEXH in cross section along six {001} planes. (c) Corresponding image from RXFH. The fluorescing Fe atom is located at the centers of the cubes in (a), (b) and (c). (d) Enlarged reconstructed image from MEXH in the (001) plane. (e) Corresponding enlarged image from RXFH. The true atomic positions of Fe and Ni atoms are shown as circles and squares, respectively, and certain key atomic positions are also labelled.

Spin-resolved electronic structure studies of ultrathin films of Fe on singular and vicinal GaAs

M. Spangenberg[1], E.A. Seddon[1], E.M.M. McCash[2], T. Shen[3],
S.A. Morton[4], D. Waddill[5] and J. Tobin[4]

[1]CLRC Daresbury Laboratory, Keckwick Lane, Daresbury, Cheshire, UK
[2]Department of Chemistry, University of York, Heslington, York, UK
[3]Joule Physics Laboratory, University of Salford, Salford, Greater Manchester, UK
[4]Lawrence Livermore National Laboratory, 7000 East Ave., Livermore, CA 94550
[5]Department of Physics, University of Missouri-Rolla, Rolla, MO 65409

Recently, there has been considerable interest in the study of spin injection at ferromagnetic semiconductor heterojunctions and ferromagnetic metal – semiconductor contacts[1,2,3,4]. Studies of n-type semiconductors have demonstrated spin-coherent transport over large distances[5] and the persistence of spin coherence over a sizeable time scale[6]. Clearly such investigations have been stimulated by the potential of the development of 'spintronics', electronic devices utilising the information of the electron spin states. To understand and improve the magnetic properties of ultrathin Fe films on GaAs has been the aim of many research groups over recent years. The interest in this system has both technological and fundamental scientific motivations. Technologically, Fe on GaAs may serve to realize spin electronic devices. From a fundamental science point of view, Fe on GaAs serves as a prototype for studies of the interplay between the crystalline structure and morphology of an ultrathin film, its electronic structure and the long range magnetic order it exhibits.

In contrast to the attention given to Fe on variously prepared GaAs substrates, the magnetism of Fe on vicinal GaAs substrates has received scant attention. This in spite of the fact that films grown on vicinal substrates present a number of advantages and opportunities. For example, they are known to exhibit enhanced structural homogeneity, surface diffusion tends to follow well mapped patterns (the quasi-periodicity has been exploited to produce quantum wires) and there is an additional degree of control of the film growth beyond those associated with temperature and substrate surface composition[7].

In a preliminary combined spin-polarized secondary electron spectroscopy, photoelectron spectroscopy and LEED study (carried out on the SRS, Daresbury Laboratory) of the remanent magnetic properties of Fe on singular and vicinal (3° offset) GaAs we have shown both that the various magnetic phases formed are dependant upon the Ga to As surface composition of the substrate and that they evolve in characteristic (but not well understood) ways with Fe overlayer thickness[8]. A remarkable feature in this system, which illustrates the importance of the Fe overlayer/substrate interaction, is the magnetic anisotropy; the easy axis of the Fe films on Ga-terminated substrates is perpendicular to that for As-terminated substrates[9,10].

These measurements were followed up with combined spin-resolved photoemission and magnetic linear dichroism experiments on Fe deposited on vicinal (offcut by 3º and 6º) or singular GaAs substrates on Beamline 7 at the ALS in collaboration with Elaine Seddon of CCLRC Daresbury Laboratory, Dan Waddill of The University of Missouri-Rolla and James Tobin Of Lawrence Livermore National Laboratory. The GaAs(100) substrates were available for film deposition at room temperature after substrate decapping *in-situ* (by thermal annealing),

at the ALS. By mounting both singular and vicinal GaAs substrates on the same sample tile the same growth conditions applied for both films facilitating direct comparison. The surface quality was monitored using LEED. The following data were obtained, high resolution spin-integrated valence bands, the spin-resolved valence bands and their energy dispersion, the film thickness dependence of the spin-resolved valence bands, magnetic linear dichroism data on the Fe3p and Fe2p core levels at a variety of photon energies.

The experiments, which were performed with Dr. Simon Morton and Dr. Jim Tobin in November of 2000 have produced considerable amount of interesting results. The significant differences in the spin-resolved valence bands between *ca.*20 Å thick Fe films on singular and vicinal (3º) GaAs are illustrated in Fig.1. As the terrace width is *ca.*55 Å the spectral differences are not due to step-localized features.

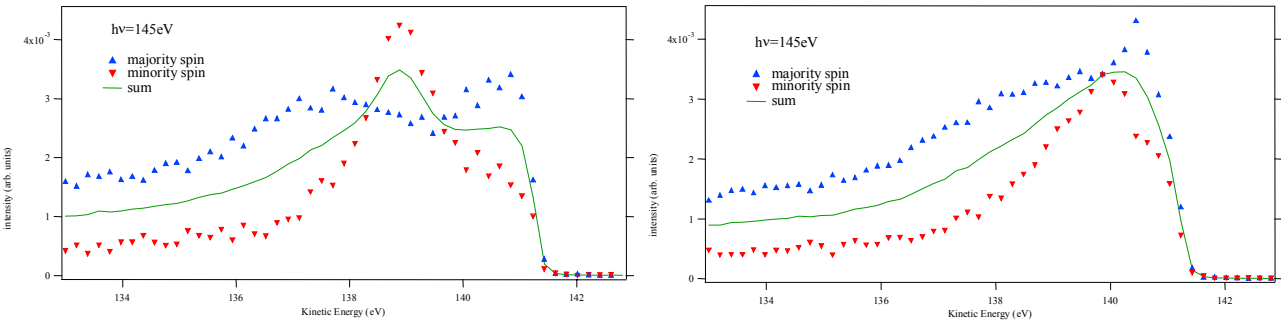

Figure 1
Spin-resolved valence band photoemission results for Fe on singular GaAs (left) and Fe on vicinal (3º) GaAs (right).

Other interesting results include the following. At low film thicknesses, Fe deposited on singular substrates was found to have a lower Curie temperature than Fe on vicinal substrates. Fe deposited on singular substrates reveals a larger energy dispersion of the spin-resolved valence bands than Fe on vicinal substrates. Only marginal differences can be seen between the spin-resolved valence bands of Fe deposited on 3º stepped GaAs substrates and Fe deposited on 6º stepped GaAs substrates. Also, in contrast to the valence band studies, the linear magnetic dichroism results obtained for these samples are very similar.

Further experiments at ALS during oct 2001 enabled us to obtain considerably more interesting results. Whilst the detailed analysis of the results is still underway, Fig.2 shows a large contrast of the valence band spectra of Fe versus incident photon energy between that on a singular and a vicinal substrate. The strong feature on the left in Fig.2 was found to be sensitive to the thickness of the Fe layer and the origin of which is still not yet clear at the present stage.

In summary, the experiments at the ALS have been extremely rewarding. They have answered some questions, clarified our thinking on others and raised yet other questions for which we have no answers at the moment. The run has, however, shown that further access to the ALS is needed to fully understand this fundamental and technologically important system.

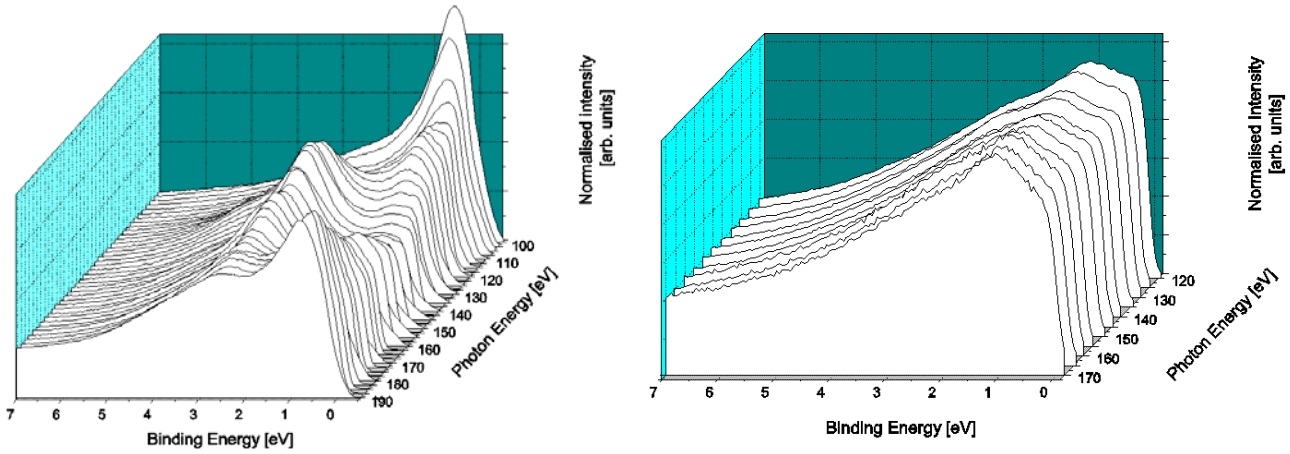

Figure 2.
Valence band spectra of Fe, normalised to the secondary electron tails, versus photon energy for films on singular substrate (left) and on 6 degree vicinal substrate (right).

References:

[1] Malajovich I., Berry J.J., Samarth N. and Awschalom D.D., Nature 411, 770 (2001)
[2] Ohno Y., Young D.K., Beschoten B., Matsukura F., Ohno H. and Awschalom D.D., Nature 402, 790 (1999)
[3] Filip A.T., Hoving B.H., Jedema F.J., van Wees B.J., Dutta B. and Borghs S., Phys. Rev. B 62, 9996 (2000)
[4] Hammar P.R., Bennett B.R., Yang M.Y. and Johnson M., Phys. Rev. Lett. 83, 203 (1999)
[5] Kikkawa J.M. and Awschalom D.D., Nature 397, 139 (1999)
[6] Kikkawa J.M. and Awschalom D.D., Phys. Rev. Lett. 80, 4313 (1998)
[7] Joyce B. A., Neave J. H., Zhang J., Vvedensky D. D., Clarke S., Hugill K.J., Shithara T. and Myers-Beaghton A.K., Semicond. Sci. Technol., **5** 1147 (1990). Kawamura T., Maruta J. and Ishii A., J. Appl. Phys., **39** (7B) 4376 (2000). Gaines J.M., Petroff P.M., Kroemer H., Simes R.J., Geels R.S. and English J.H., J. Vac. Sci. Technol., **B6** 1373 (1998).
[8] Zhang T., Spangenberg M., Greig D., Takahashi N., Shen T-H., Matthew J.A.D., Cornelius S. M., Rendall M. and Seddon, E.A., Appl. Phys. Letters, **78** 961 (2001)
[9] Kneedler E. M., Jonker B. T., Thibado P. M., Wagner R. J., Shanabrook B. V., and Whitman L., J. Phys. Rev. B, **56** 8163 (1997).
[10] Gester M., Daboo C., Hicken R. J., Gray S. J., Ercole A., and Bland J. A. C., J. Appl. Physics **80** 347 (1996).

This work was supported by the Director, Office of Energy Research, Office of Basic Energy Sciences, Materials Science Division, of the U.S. Department of Energy under Contract No. # R5-32633.A02. This work was performed under the auspices of the U.S Department of Energy by Lawrence Livermore National Laboratory under contract no. W-7405-Eng-48. Experiments were carried out at the Spectromicroscopy Facility (Beamline 7.0) at the Advanced Light Source, built and supported by the Office of Basic Energy Science, U.S. Department of Energy.

Principal investigator: E. A. Seddon, CCLRC Daresbury Laboratory, Daresbury, Warrington Cheshire, WA4 4AD, UK, Email: e.a.seddon@dl.ac.uk, Telephone: +44 1925 603245, fax +44 1925 693124